Electronic Supplementary Material (ESI) for Materials Advances.

Supplementary Information

Photo-energy Conversion Efficiency of $CH_3NH_3PbI_3/C_{60}$ Heterojunction Perovskite Solar Cells from First-principles

Khian-Hooi Chew,[1] Riichi Kuwahara,[2] and Kaoru Ohno[3]

[1]*Department of Physics, University of Malaya, 50603 Kuala Lumpur, Malaysia.*

[2]*Dassault Systèmes, ThinkPark Tower, 2-1-1 Osaki, Shinagawa-ku, Tokyo 141-6020, Japan*

[3]*Department of Physics, Yokohama National University, 79-5 Tokiwadai, Hogogaya-ku, Yokohama 240-8501, Japan.*

Section 1: Summarized of numerical values in tables

Table S1. Calculated total DFT-D energy and the relative energies of a $CH_3NH_3PbI_3/C_{60}$ heterojunction with tetragonal and cubic perovskites.

Surface geometry	Location of C_{60} on $MAPbI_3$ surface	tetragonal $MAPbI_3$ (*t*-MAI)		cubic $MAPbI_3$ (c-MAI)	
		Total DFT-D energy [eV]	Total energy relative to the topC (*t*-MAI) [eV]	Total DFT-D energy [eV]	Total energy relative to the topC (*t*-MAI) [eV]
topC	aboveC	-33358486.71	0.000	-33358486.1	0.610
	aboveI	-33358486.02	0.696	-	-
	bridge	-33358486.54	0.176	-33358484.08	2.636
topN	aboveN	-33358483.92	2.792	-33358485.28	1.437
	aboveI	-33358484.16	2.556	-33358486.05	0.659
	bridge	-33358483.83	2.884	-33358485.29	1.420
apolar	aboveC	-33358484.73	1.988	-33358485.45	1.262
	aboveN	-33358484.84	1.878	-33358485.2	1.513
	aboveI	-33358484.78	1.931	-33358485.61	1.101
	bridge	-33358484.83	1.887	-33358486.26	0.455

Table S2. Calculated energy gap E_g, the dissociated energy of the electron-hole pair ΔE and energy conversion efficiency η of a $CH_3NH_3PbI_3/C_{60}$ heterojunction with tetragonal-phase perovskites. ΔE^* and η^* denote the dissociated energy and the energy conversion efficiency obtained based on the three-fold degenerate LUMO of C_{60} fullerene.

Surface geometry	Location of C_{60} on $MAPbI_3$	E_g [eV]	ΔE [eV]	η [%]	ΔE^* [eV]	η^* [%]
topC	aboveC	1.715	0.704	14.22	0.693	14.43
	aboveI	1.409	0.484	18.72	0.467	19.21
	bridge	1.677	0.651	15.29	0.646	15.41
topN	aboveN	1.497	0.909	0	0.891	0
	aboveI	1.51	0.945	0	0.913	0
	bridge	1.495	0.921	0	0.890	0
apolar	aboveC	1.642	0.984	0	(0.963	0
	aboveN	1.556	0.839	0	0.824	0
	aboveI	1.604	0.944	0	0.926	0
	bridge	1.587	0.894	0	0.880	0

Table S3. Calculated energy gap E_g, the dissociated energy of the electron-hole pair ΔE and energy conversion efficiency η of a $CH_3NH_3PbI_3/C_{60}$ heterojunction with cubic-phase perovskites. ΔE^* and η^* denote the dissociated energy and the energy conversion efficiency obtained based on the three-fold degenerate LUMO of C_{60} fullerene.

Surface geometry	Position of C_{60} on $MAPbI_3$	E_g [eV]	ΔE [eV]	η [%]	ΔE^* [eV]	η^* [%]
topC	aboveC	1.968	0.943	9.97	0.918	10.32
	aboveI	0	0	0	0	0
	bridge	1.895	0.828	11.82	0.806	12.16
topN	aboveN	1.874	0.985	9.32	0.970	9.55
	aboveI	1.737	0.947	8.88	0.924	9.92
	bridge	1.764	0.929	9.99	0.901	10.50
apolar	aboveC	1.877	0.975	9.48	0.948	9.91
	aboveN	1.881	0.954	9.84	0.938	10.09
	aboveI	1.846	0.963	9.64	0.950	9.86
	bridge	1.916	0.987	9.36	0.959	9.78

Table S4. Calculated binding energies of a $CH_3NH_3PbI_3/C_{60}$ heterojunction with tetragonal and cubic perovskites.

Surface geometry	Location of C_{60} on $MAPbI_3$ surface	tetragonal $MAPbI_3$ (*t*-MAI)	cubic $MAPbI_3$ (*c*-MAI)
		binding energy [eV]	binding energy [eV]
topC	aboveC	-1.717	-4.658
	aboveI	-1.021	-
	bridge	-1.541	-2.631
topN	aboveN	-2.737	-6.063
	aboveI	-2.973	-6.840
	bridge	-2.645	-6.080
apolar	aboveC	-2.231	-5.026
	aboveN	-2.341	-4.774
	aboveI	-2.288	-5.187
	bridge	-2.333	-5.833

Section 2: Optimized structures of $MAPbI_3/C_{60}$ heterojunctions

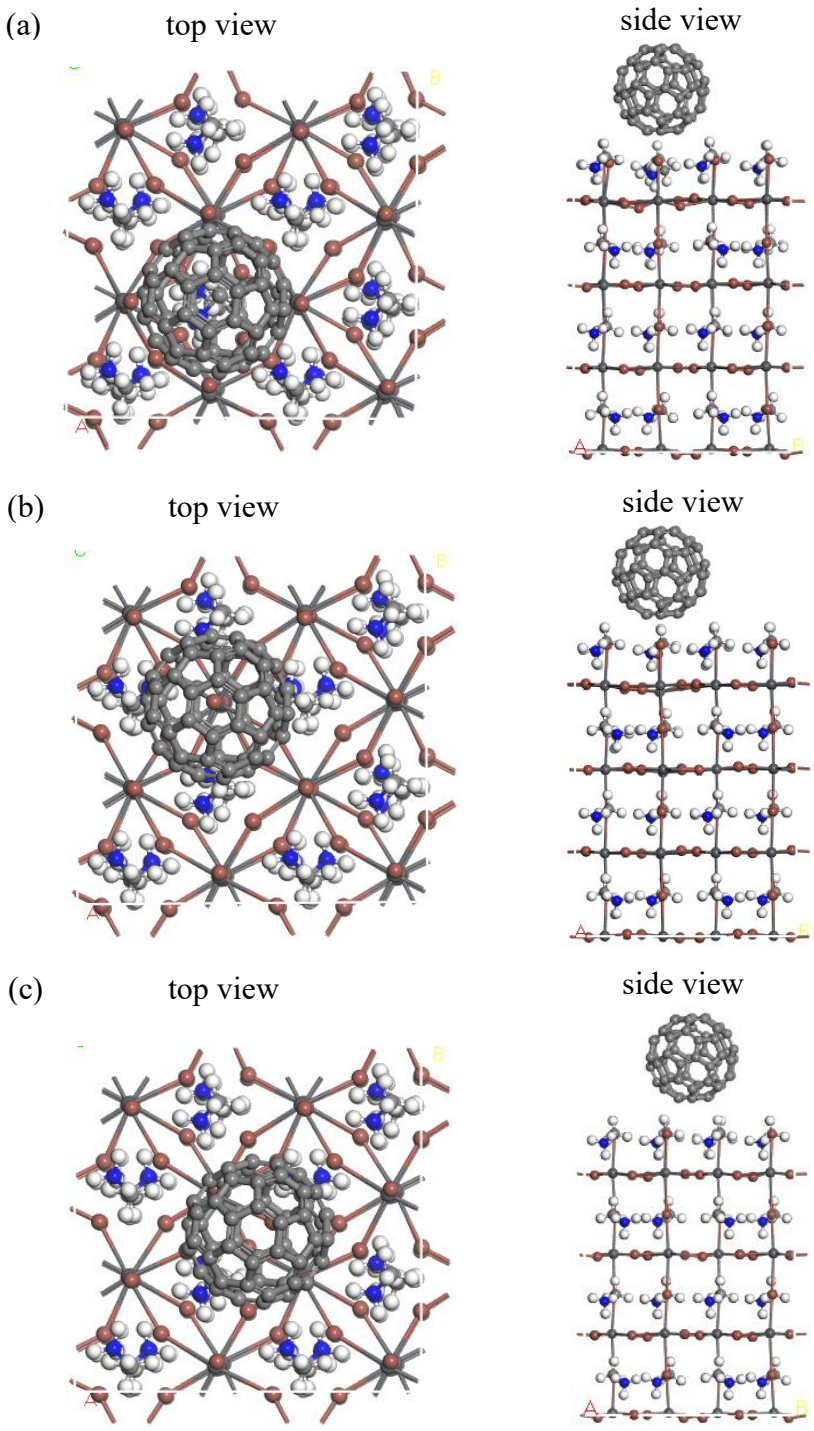

Figure S1. Optimized structures of a $MAPbI_3/C_{60}$ heterojunction with tetragonal-phase perovskites. The perovskite has a topC geometry with a fullerene C_{60} on the (a) aboveC, (b) aboveI and (c) bridge positions. H, C, N, I, and Pb atoms are represented by the white, light grey, blue, brown, and dark grey spheres, respectively.

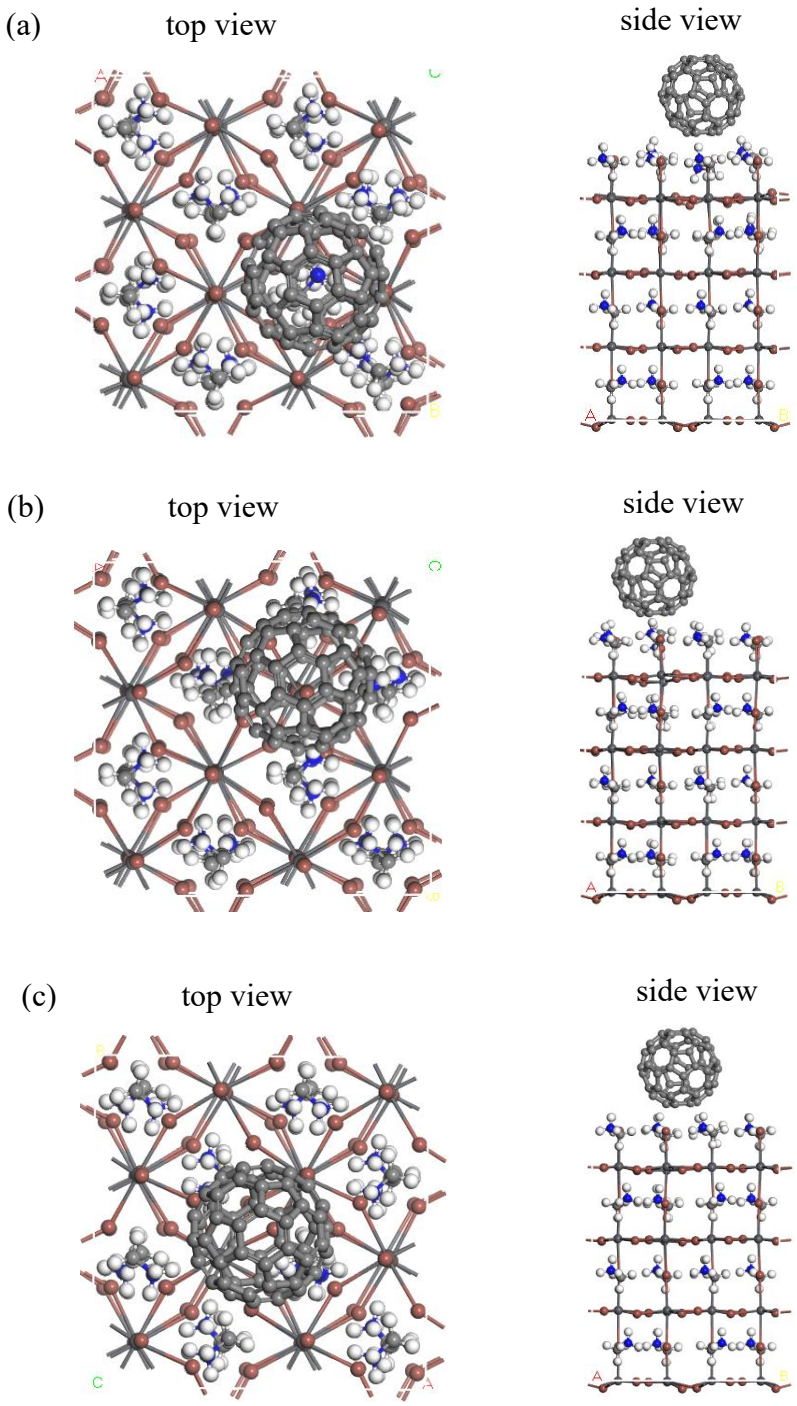

Figure S2. Optimized structures of a $MAPbI_3/C_{60}$ heterojunction with tetragonal-phase perovskites. The perovskite has a topN geometry with a fullerene C_{60} on the (a) aboveN, (b) aboveI and (c) bridge positions. H, C, N, I, and Pb atoms are represented by the white, light grey, blue, brown, and dark grey spheres, respectively.

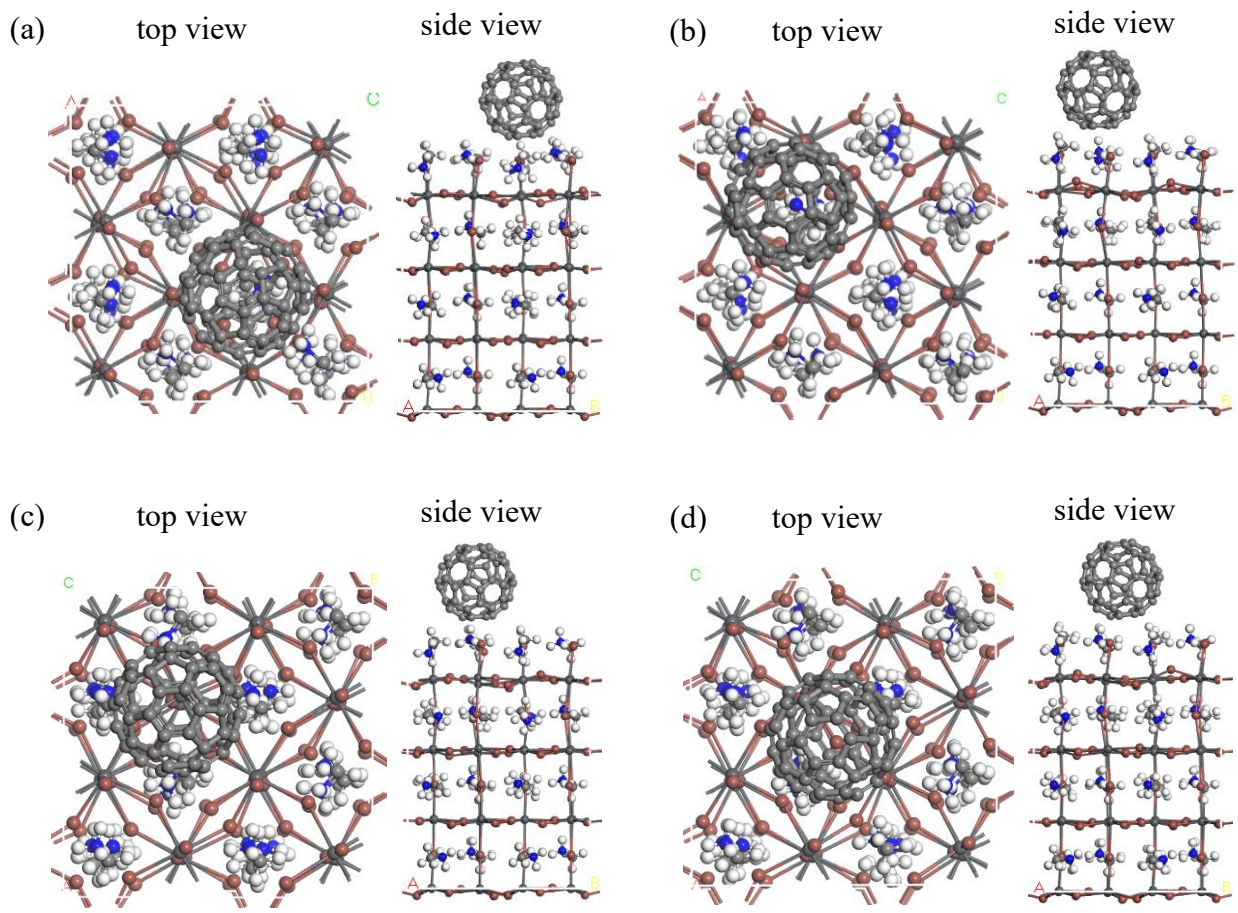

Figure S3. Optimized structures of a $MAPbI_3/C_{60}$ heterojunction with tetragonal-phase perovskites. The perovskite has an apolar orientation with a fullerene C_{60} on the (a) aboveC, (b) aboveN, (b) aboveI and (c) bridge positions. H, C, N, I, and Pb atoms are represented by the white, light grey, blue, brown, and dark grey spheres, respectively.

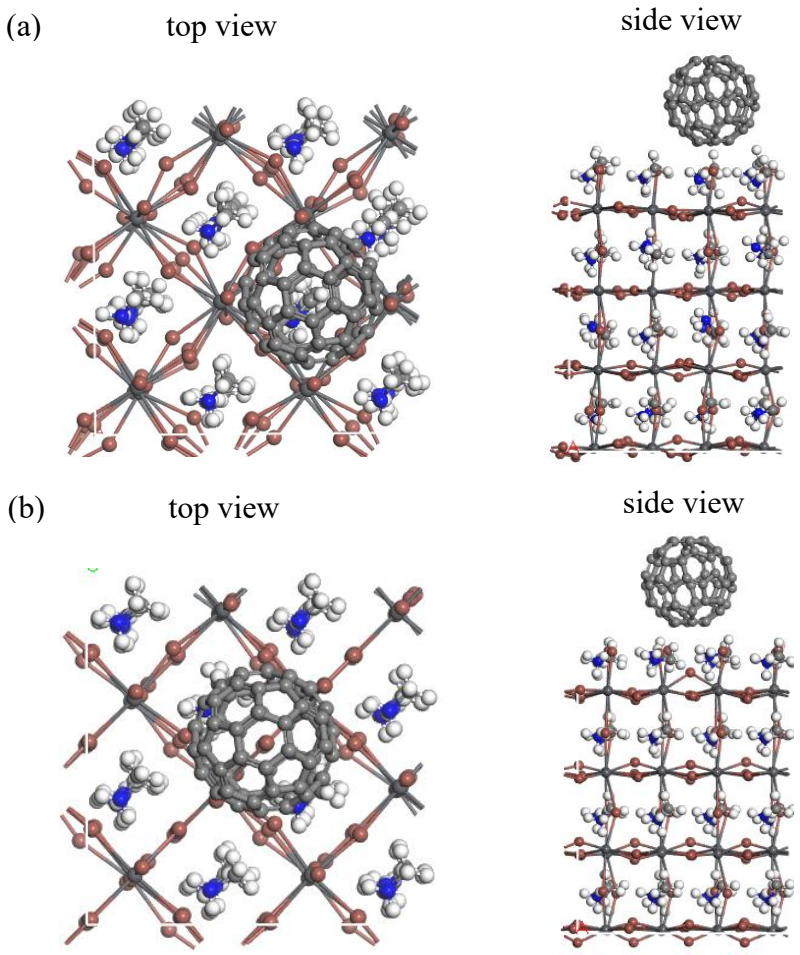

Figure S4. Optimized structures of a $MAPbI_3/C_{60}$ heterojunction with cubic-phase perovskites. The perovskite has a topC geometry with a fullerene C_{60} on the (a) aboveC and (b) bridge positions. H, C, N, I, and Pb atoms are represented by the white, light grey, blue, brown, and dark grey spheres, respectively.

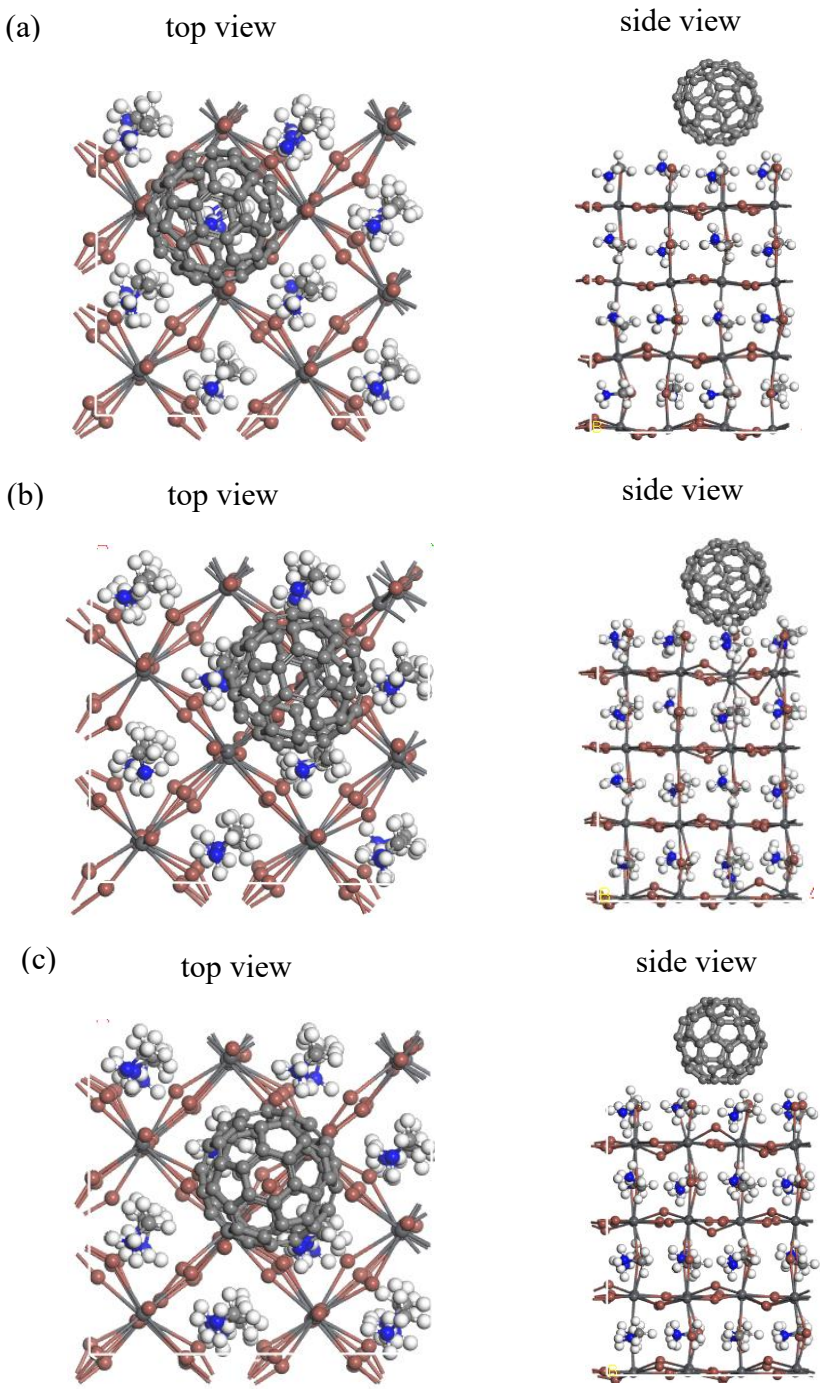

Figure S5. Optimized structures of a $MAPbI_3/C_{60}$ heterojunction with cubic-phase perovskites. The perovskite has a topN geometry with a fullerene C_{60} on the (a) aboveN, (b) aboveI and (b) bridge positions. H, C, N, I, and Pb atoms are represented by the white, light grey, blue, brown, and dark grey spheres, respectively.

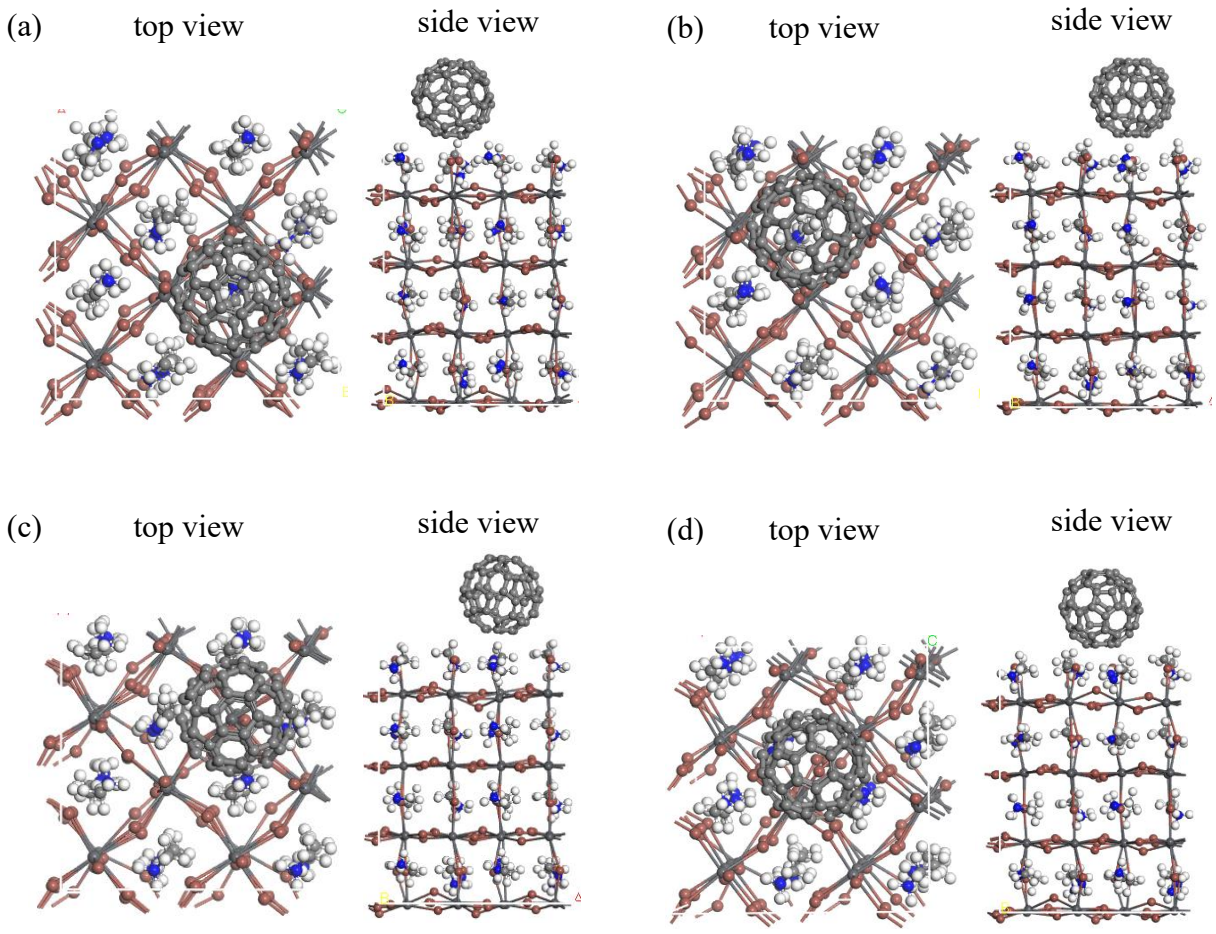

Figure S6. Optimized structures of a $MAPbI_3/C_{60}$ heterojunction with cubic-phase perovskites. The perovskite has apolar geometry with a fullerene C_{60} on the (a) aboveC, (b) aboveN, (c) aboveI and (d) bridge positions. H, C, N, I, and Pb atoms are represented by the white, light grey, blue, brown, and dark grey spheres, respectively.

Section 3: Kohn-Sham orbitals and energy eigenvalues of $MAPbI_3/C_{60}$ heterojunctions

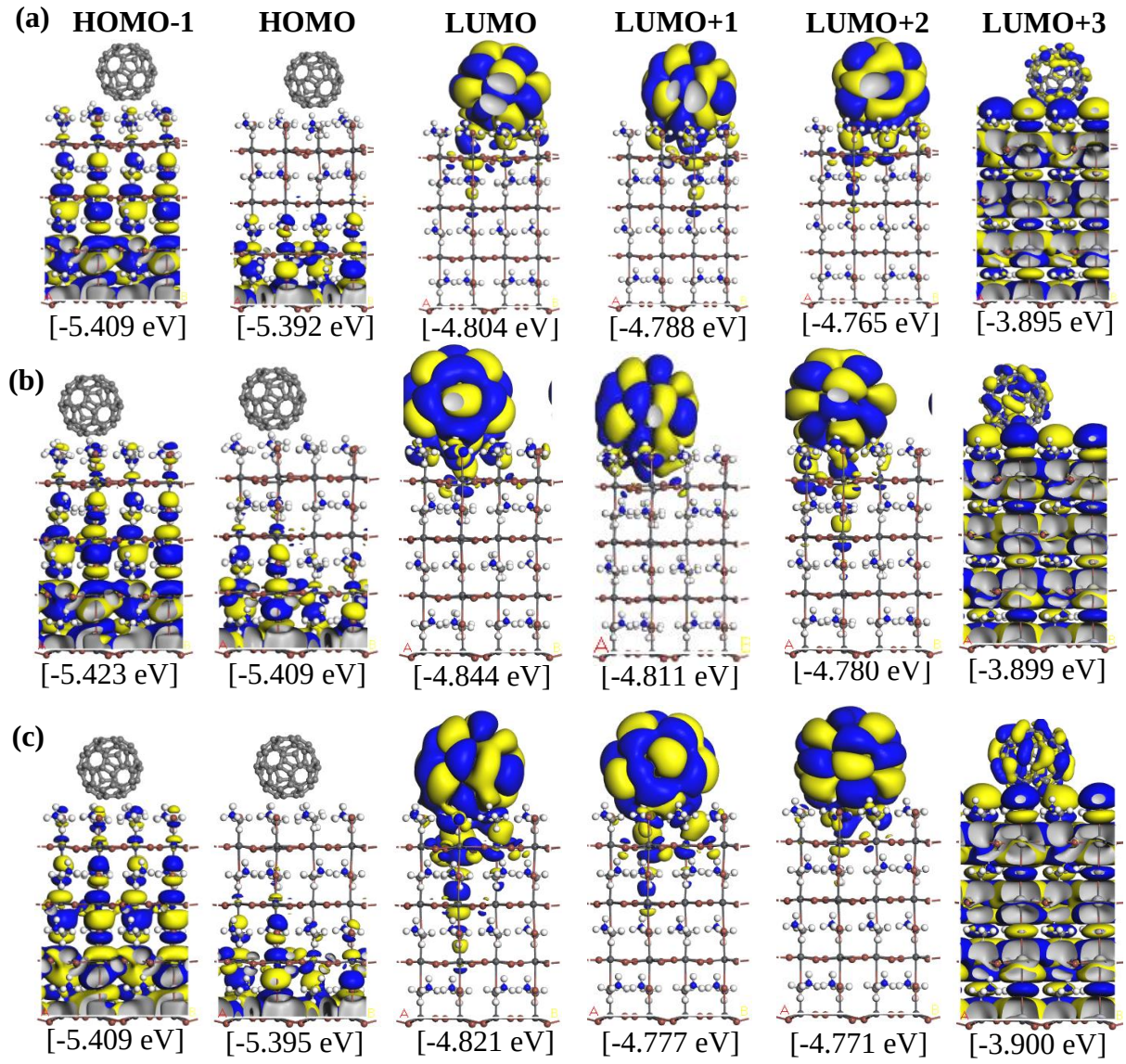

Figure S7. Calculated Kohn-Sham orbitals and energy eigenvalues of a $MAPbI_3/C_{60}$ heterojunction with tetragonal $MAPbI_3$ from HOMO-1 to LUMO+3 levels. Yellow and blue denote plus and minus region of the orbitals. The perovskite has a topN orientation with a fullerene C_{60} on the (a) aboveC, (b) aboveI and (c) bridge positions.

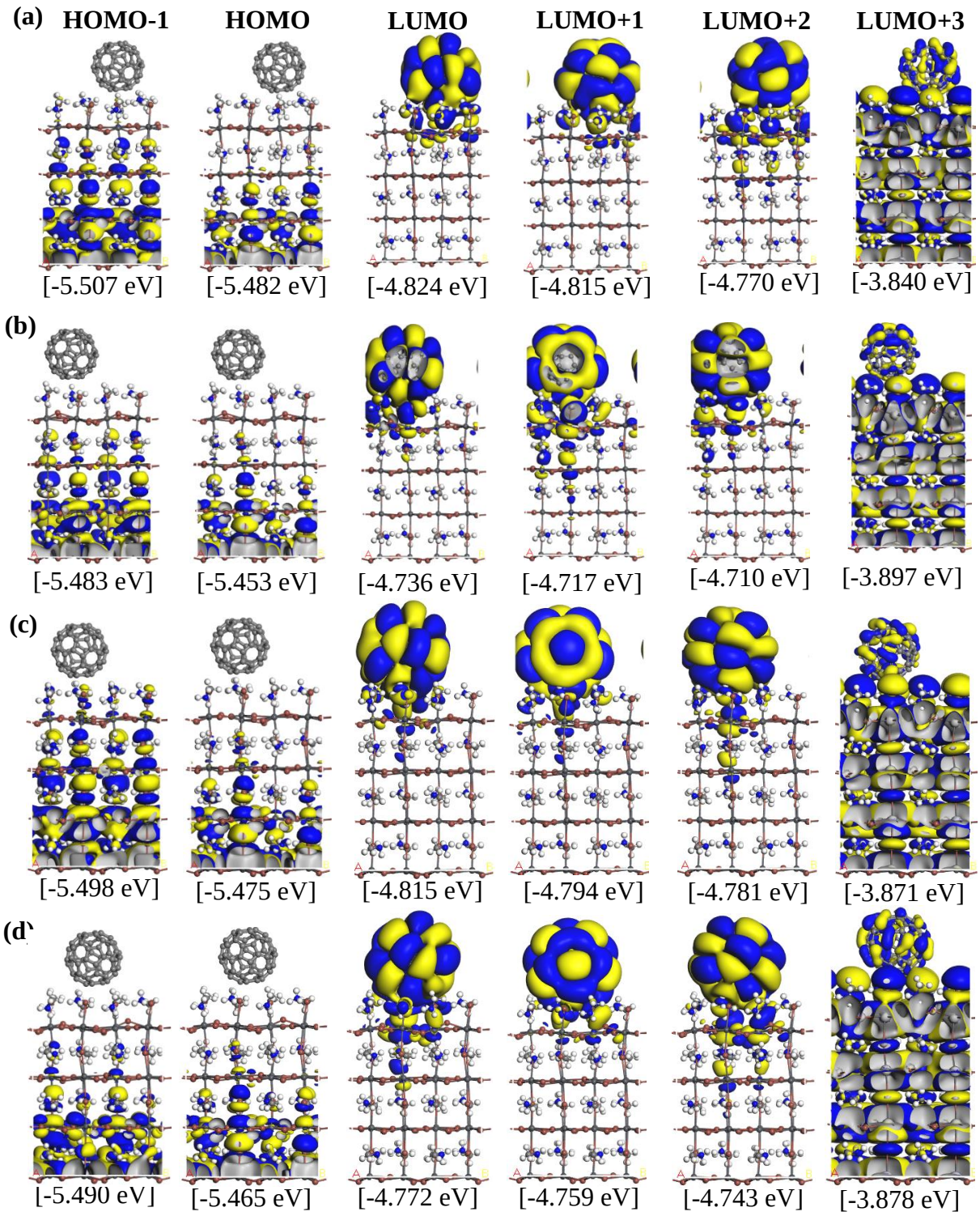

Figure S8. Calculated Kohn-Sham orbitals and energy eigenvalues of a $MAPbI_3/C_{60}$ heterojunction with tetragonal $MAPbI_3$ from HOMO-1 to LUMO+3 levels. Yellow and blue denote plus and minus region of the orbitals. The perovskite has an apolar orientation with a fullerene C_{60} on the (a) aboveC, (b) aboveN, (c) aboveI and (d) bridge positions.

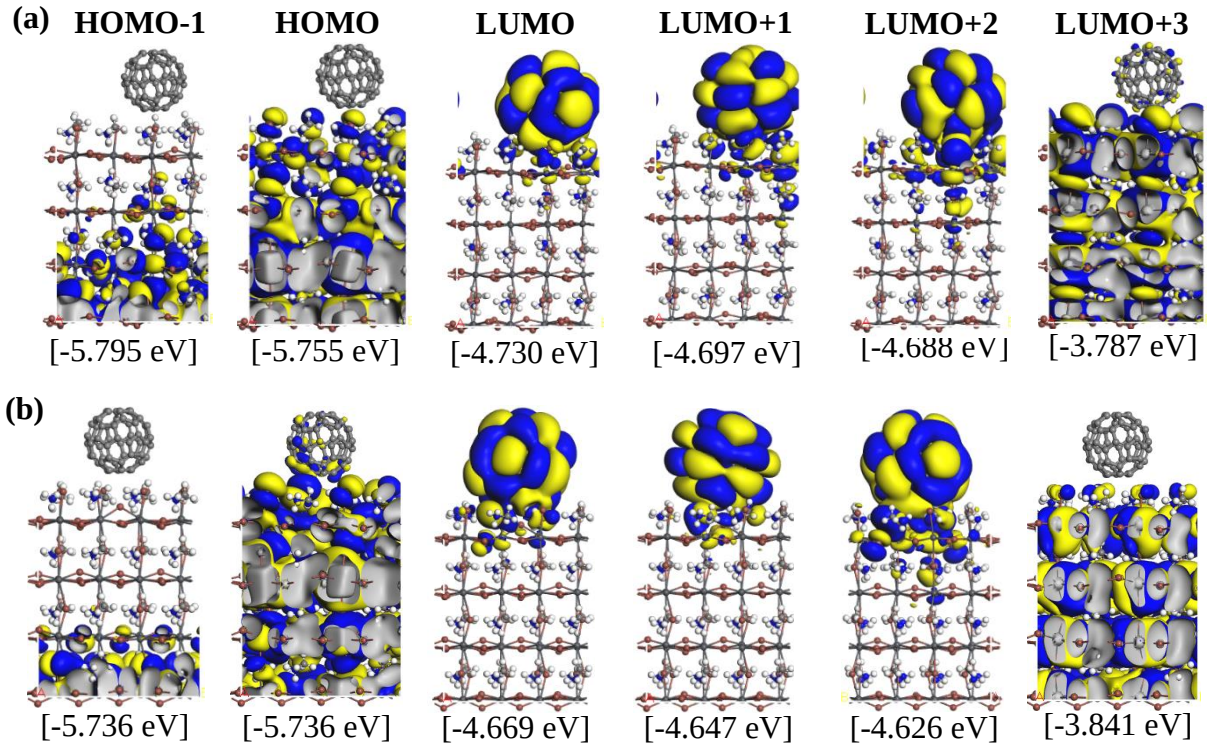

Figure S9. Calculated Kohn-Sham orbitals and energy eigenvalues of a $MAPbI_3/C_{60}$ heterojunction with cubic $MAPbI_3$ from HOMO-1 to LUMO+3 levels. The perovskite has a topC geometry with a fullerene C_{60} on the (a) aboveC and (b) bridge positions.

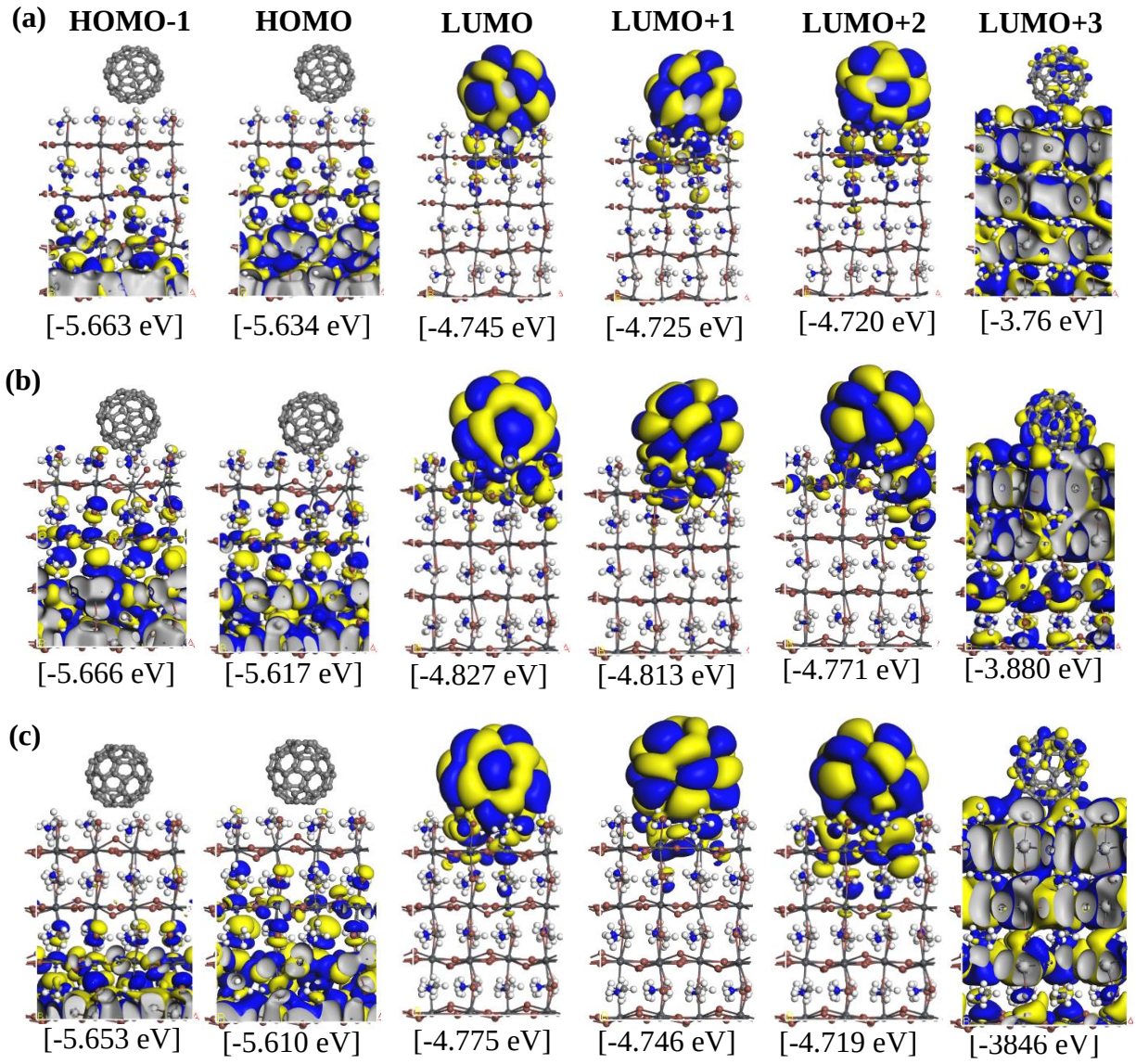

Figure S10. Calculated Kohn-Sham orbitals and energy eigenvalues of a $MAPbI_3/C_{60}$ heterojunction with cubic $MAPbI_3$ from HOMO-1 to LUMO+3 levels. The perovskite has a topN geometry with a fullerene C_{60} on the (a) aboveN, (b) aboveI and (c) bridge positions.

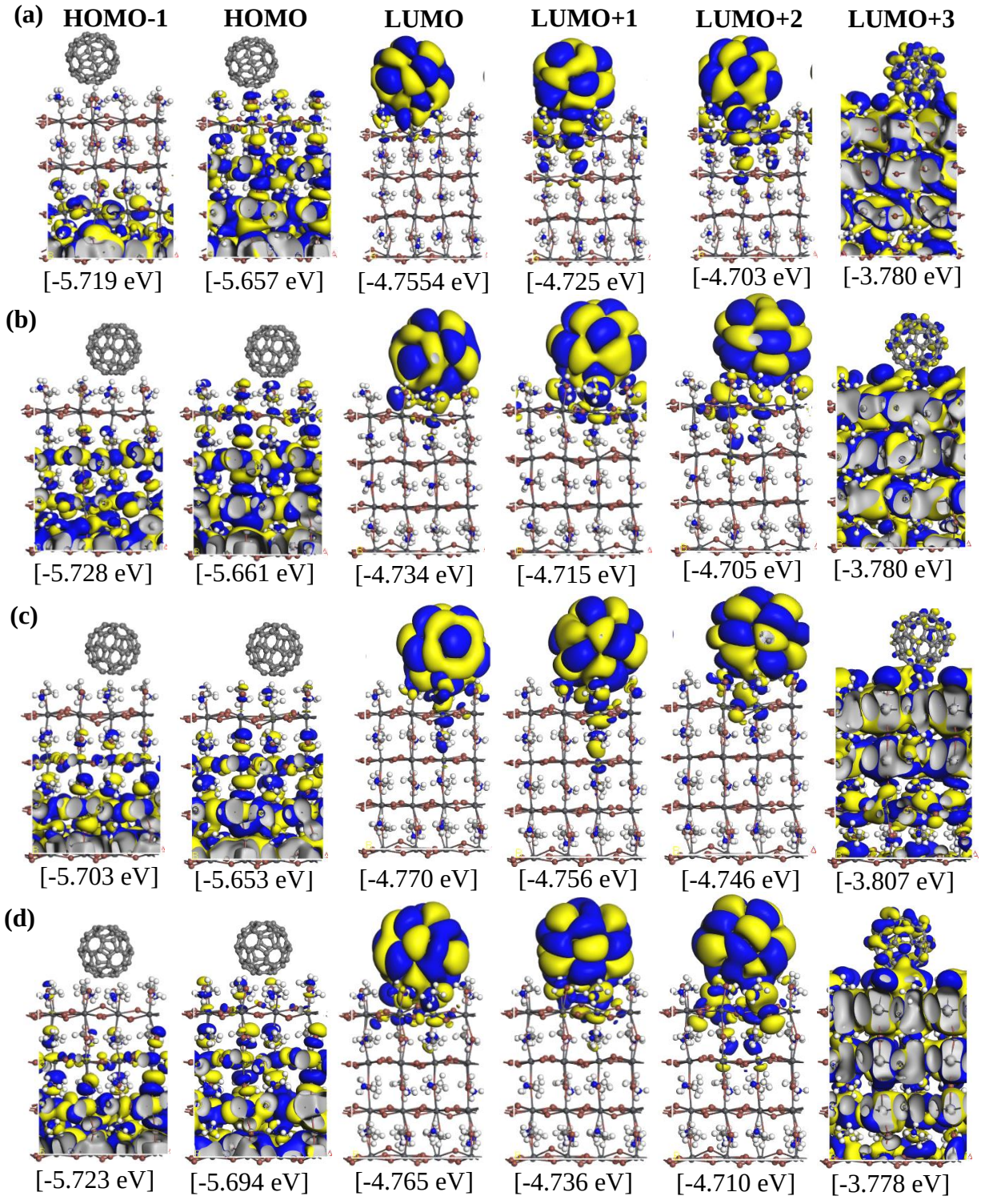

Figure S11. Calculated Kohn-Sham orbitals and energy eigenvalues of a $MAPbI_3/C_{60}$ heterojunction with cubic $MAPbI_3$ from HOMO-1 to LUMO+3 levels. The perovskite has an apolar geometry with a fullerene C_{60} on the (a) aboveC, (b) aboveN, (c) aboveI and (d) bridge positions.